A GENERALIZED TWO-LEVEL GRAPHICAL FORECAST SCHEME

T. N. KRISHNAMURTI

Department of Meteorology, University of California, Los Angeles, Calif.

[Manuscript received March 14, 1962; revised April 25, 1962]

ABSTRACT

An arbitrary isobaric surface and the level of non-divergence constitute the two levels of the proposed model. The vorticity equation consistent with the quasi-geostrophic assumptions is applied at two levels. The thermodynamic energy equation for adiabatic motion is applied to the layer between the two levels. A parabolic profile for the vertical motion is assumed. The vertical motion is eliminated between the vorticity and the thermodynamic energy equations to obtain prognostic equations. The prognostic equations are solved by a generalized graphical forecast scheme of successive approximations. Forecasts and forecast errors in a selected meteorological situation are discussed.

1. INTRODUCTION

The barotropic forecast scheme of Fjørtoft [2], [3] was extended to a simple baroclinic model by Estoque [1]. The latter dealt with a model between the 1,000 and the 500-mb. surfaces. The 500-mb. forecasts were made with the barotropic model, and a simple thickness advection scheme yielded the 1,000-mb. forecasts. It will be our attempt to generalize a two-level model that may be applicable between the level of non-divergence and any other level. In particular, we shall attempt to apply the theory to forecast the 300-mb. height field in a selected situation.

In the modern age of high-speed computers it is difficult to place the importance of graphical forecasts when corresponding numerical forecast models are in operation. Petterssen's [7] view on this is perhaps still pertinent: "The general aspects of the graphical integration procedure is of considerable interest; apart from being economical in manpower, it is highly transparent and enables the forecaster to remain in touch with the problem through all stages of its solution. It is relatively easy, therefore, to identify assumptions and simplifications which contribute to satisfactory and unsatisfactory results." The two-level simple baroclinic model proposed here is initiated with this in view.

In this connection it may be added that the earlier work of Fjørtoft on his barotropic and baroclinic graphical forecast models [2], [3] led to several quasi-Lagrangian numerical forecast models (Wiin-Nielsen [10], Sawyer [9], and Oakland [6]). In Oslo, some operational numerical forecast models are being carried out utilizing essentially Fjørtoft's graphical forecast models where one uses large time steps of the order of 6 hours.

2. THE BASIC EQUATIONS OF THE MODEL

Let subscript 1 refer to an arbitrary level in the atmosphere and 2 to the level of non-divergence.

Consistent with the assumptions pertinent to quasi-geostrophic systems the following terms of the vorticity equations are omitted: the vertical advection terms, the twisting terms, relative vorticity in the divergence term, and any frictional contributions.

The vorticity equations at levels 1 and 2 may be written as

$$\left(\frac{\partial}{\partial t}+\mathbf{V}_1\cdot\nabla\right)(\zeta_1+f)=-f\nabla\cdot\mathbf{V}_1 \tag{1}$$

$$\left(\frac{\partial}{\partial t}+\mathbf{V}_2\cdot\nabla\right)(\zeta_2+f)=0 \tag{2}$$

where ζ is the vertical component of relative vorticity, $\mathbf{V}$ is the wind vector, f is the Coriolis parameter, and t is time. ζ_1 and ζ_2 and the advection of vorticity are evaluated with the geostrophic winds.

The thermodynamic energy equation for adiabatic motion may be written, with the aid of the hydrostatic equation in the form:

$$\left(\frac{\partial}{\partial t}+\mathbf{V}\cdot\nabla\right)\frac{\partial z}{\partial p}=\sigma\omega$$

where z is height, p is pressure, $\omega\equiv dp/dt$, and σ is static stability. It is convenient to express $\partial z/\partial p$ by either its finite difference equivalent expression $(z_1-z_2)/(p_1-p_2)$, or if the hodograph of the wind between levels 1 and 2 is assumed to be straight, we may write the adiabatic relation in the form

$$\left(\frac{\partial}{\partial t}+\mathbf{V}_2\cdot\nabla\right)H=\sigma(p_1-p_2)\,\omega_m \tag{3}$$

where ω_m refers to a mean value of ω for the layer of thickness H.

Equations (1), (2), and (3) are the principal equations of the model for the three unknowns z_1, z_2, and ω. A constant value of the static stability σ is assumed.

3. THE PARABOLIC VERTICAL VELOCITY PROFILE

Reed [8] utilized a linear vertical velocity profile in his discussion of a two-level baroclinic model between the surface and the 500-mb. surface. Knighting's [4] work has more conclusively shown that the use of a parabolic profile is not a bad approximation. Using multilevel quasi-geostrophic models, he found that the vertical motion profile over large portions of the map indeed had the parabolic form. Estoque [1] utilized a sinusoidal vertical velocity profile in his work.

Assuming an equation of the form:

$$\omega=ap^2+bp+c$$

we shall impose the following boundary conditions on ω:

$\omega=0$ at 1,000 mb.
$\omega=0$ at 0 mb.
$\omega=\omega_2$ at the level of non-divergence

With these boundary conditions we may write:

$$\omega=(a_1p^2+b_1p+c_1)\omega_2 \tag{4}$$

where a_1, b_1, and c_1 have respectively the magnitudes $(-1/250{,}000)$, $(1/250)$, (0), where the unit of pressure is a millibar.

It is now possible to express the divergence term of equation (1) and ω_m in terms of the ω profile given by equation (4)

$$-f\nabla\cdot\mathbf{V}_1=f\left(\frac{\partial\omega}{\partial p}\right)_1=f(2a_1p_1+b_1)\omega_2$$

$$\omega_m=\frac{\int_{p_1}^{p_2}\omega dp}{\int_{p_1}^{p_2}dp}=\left\{\frac{a_1}{3}(p_1^2+p_1p_2+p_2^2)+\frac{b_1}{2}(p_1+p_2)+c_1\right\}\omega_2$$

Introducing two new variables l and h we may write

$$-f\nabla\cdot\mathbf{V}_1=l\omega_2$$

$$\omega_m=h\omega_2$$

Further, let $k=(p_1-p_2)h\sigma$. Equations (1), (2), and (3) may now be written in terms of ω_2:

$$\left(\frac{\partial}{\partial t}+\mathbf{V}_1\cdot\nabla\right)\left(\frac{g}{f}\nabla^2z_1+f\right)=l\omega_2 \tag{5}$$

$$\left(\frac{\partial}{\partial t}+\mathbf{V}_2\cdot\nabla\right)\left(\frac{g}{f}\nabla^2z_2+f\right)=0 \tag{6}$$

$$\left(\frac{\partial}{\partial t}+\mathbf{V}_2\cdot\nabla\right)H=k\omega_2 \tag{7}$$

4. THE PREDICTION EQUATIONS AND THE SUCCESSIVE APPROXIMATION SCHEME

In all such formulations of the simple baroclinic models, one eliminates the vertical velocity and obtains prognostic equations for z_1 and z_2. We shall proceed in this conventional manner and eliminate ω_2. Further, we shall obtain prognostic equations for z_1 and z_2 in the manner of Fjørtoft [3] and Estoque [1], however, retaining all of the advection terms.

Subtract (6) from (5) and substitute for ω_2 from (7) in the resulting equation, and we obtain:

$$\left(\frac{\partial}{\partial t}+\mathbf{V}_2\cdot\nabla\right)\left(\frac{g}{f}\nabla^2H-\frac{l}{k}H\right)=-(\mathbf{V}_1-\mathbf{V}_2)\cdot\nabla\left(\frac{g}{f}\nabla^2z_1+f\right) \tag{8}$$

Equations (6) and (8) are the prediction equations.

Equation (6) may be solved by the conventional relaxation method or by Fjørtoft's well known graphical forecast scheme. We shall assume here that equation (6) has been solved by one of these methods and that we now have the solution for say, the next 24 hours. In the following we will be interested in the solution of equation (8).

Introducing the Jacobean notation we may rewrite equation (8) as follows:

$$\frac{\partial}{\partial t}\left[\frac{g}{f}\nabla^2H-\frac{lH}{k}\right]=-\frac{g}{f}\mathbf{J}\left[z_2,\frac{g}{f}\nabla^2H-\frac{l}{k}H\right]-\frac{g}{f}\mathbf{J}\left[H,\frac{g}{f}\nabla^2z_1+f\right] \tag{9}$$

Further, writing

$$\nabla^2H=\frac{4m^2}{L^2}(\bar{H}-H)$$

and

$$\nabla^2z_1=\frac{4m^2}{L^2}(\bar{z}_1-z_1)$$

where m is a map scale factor, L is the grid-distance in a rectangular grid network and the bar refers to the mean value of H and z_1, over four surrounding points in the conventional sense.

Let

$$B=\frac{1}{1+\frac{flL^2}{4gkm^2}}$$

Equation (9) may be written in terms of B, z_1, H in the form:

$$\frac{\partial}{\partial t}(H-B\bar{H})=-\frac{g}{f}\mathbf{J}(z_2,H-B\bar{H})-\frac{g}{f}\mathbf{J}\left[H,B(z_1-\bar{z}_1)-\frac{f^2BL^2}{4gm^2}\right] \tag{10}$$

We shall attempt here to solve equation (10) by a method of successive approximations.

THE FIRST APPROXIMATION

The first approximation solution will be obtained by dropping the second term on the right hand side of equation (10). This approximation is equivalent to an assump-

tion of zero wind shear between the two levels. The quantity $(H-B\overline{H})$ is conserved, as in Estoque's [1] work, although B has a different interpretation. We shall use a superscript inside parentheses to indicate the order of the approximations:

$$\frac{\partial}{\partial t}(H^{(1)}-B\overline{H}^{(1)})=-\frac{g}{f}\mathbf{J}(z_2,H^{(1)}-B\overline{H}^{(1)}) \qquad (11)$$

Advection of $(H^{(1)}-B\overline{H}^{(1)})$ can be made for 12 hours along the initial chart of z_2 and for another 12 hours along the forecast chart of z_2 by the conventional graphical forecasting methods. The change in $H^{(1)}$ can then be recovered by a scheme as follows, Fjørtoft [3]:

Let

$$\Delta(H^{(1)}-B\overline{H}^{(1)})=Q \qquad \text{(a 24-hour change)}$$

then

$$\Delta H^{(1)}=Q+B\overline{Q}$$

We may then write

$$H_F^{(1)}=H_I+\Delta H^{(1)}$$

where H_I is the initial magnitude of thickness and $H_F^{(1)}$ is the forecast value to the first approximation.

We may then obtain

$$z_{1F}^{(1)}=z_{2F}+H_F^{(1)}$$

where z_{2F} is the forecast value of z_2, and $z_1{}_F^{(1)}$ would be the forecast value of z_1, to the first approximation.

HIGHER ORDER APPROXIMATIONS

The general form for equation (10) for $n>1$ may now be written as:

$$\frac{\partial}{\partial t}[H^{(n)}-B\overline{H}^{(n)}]=-\frac{g}{f}\mathbf{J}[z_2,H^{(n-1)}-B\overline{H}^{(n-1)}]$$
$$-\frac{g}{f}\mathbf{J}\left[H^{(n-1)},B(z_1^{(n-1)}-\overline{z}_1^{(n-1)})-\frac{f^2BL^2}{4gm^2}\right] \qquad (14)$$

In the higher order approximations the change in $(H^{(n)}-B\overline{H}^{(n)})$ is obtained by terms of one lower order approximation. This scheme is very similar to many numerical iterations of the like kind.

We may further write a 24-hour change as

$$\Delta(H^{(n)}-B\overline{H}^{(n)})=Q^{(n)}$$

and

$$\Delta H^{(n)}=Q^{(n)}+B\overline{Q}^{(n)}$$

$$H_F^{(n)}=H_I+\Delta H^{(n)} \qquad (15)$$

$$z_{1F}^{(n)}=z_{2F}+H_F^{(n)} \qquad (16)$$

Equations (15) and (16) predict the thickness and the height z_1 fields. One would be obligated to demonstrate the convergence of such a scheme of successive approximations. Such work can be carried out on an electronic computer. In the graphical forecast scheme proposed here, we shall only suggest the first few approximations; in practice these can be carried out in a laboratory in a very short time, of just over one hour. We shall partially justify the convergence of the scheme by showing that the correction terms demanded by the higher approximations are much smaller than the first approximations.

In the following section we shall show an example of a graphical forecast with illustrations of the various steps and make some comparison with the verification charts.

5. A CASE STUDY OF A WINTER STORM OVER THE CENTRAL UNITED STATES

From the files of winter synoptic situations, a case during December 31, 1959, through January 2, 1960, was selected. We shall demonstrate here a 24-hour forecast made from December 31, 1200 GMT, for January 1, 1200 GMT.

Of particular interest perhaps, is the geostrophic wind field associated with the 500-mb. chart shown in figure 1 for the initial map. A large vorticity center off the west coast of North America with a typical difluent trough characterizes the flow. (The contours are drawn for every 100 meters.) This initial chart is a synoptic situation that characterizes development from simple considerations of vorticity advection into the upper trough. The pertinent questions that we are interested in are in relation to such a development. The ridge over the Midwestern States would perhaps react to any such development and its behavior would also be of importance for the development and movement of surface phenomena.

Figure 2 shows the 500-mb. chart for January 1 at 1200 GMT. The height analysis reflects a certain amount of vorticity advection into the upper trough. The winds to the rear of the trough do not appear to be as strong. The ridge over the Midwestern States has moved eastward over the Great Lakes area without much change. The difluent characteristics of the upper trough on the 31st are not maintained at this time. To the north of the trough-ridge complex the flow has remained from the west without much change.

The barotropic prognostic chart (z_{2F}) is shown in figure 3 and is valid at the time of figure 2. The prognostic chart appears to be a very good forecast in relation to the position and intensity of the ridge and the general flow pattern. In the region of the trough barotropic development is noticeable, this being due to transformation of the earth's and shear vorticities into curvature vorticity in the strong northwest flow. The reason for this slight overestimation of the development may lie in the neglected dynamics (vertical advection, twisting effects, and in the assumption of a level of non-divergence around the 500-mb. surface). Consistent with this forecast for the level of non-divergence we shall attempt to carry out the proposed analysis for the 300-mb. surface.

The initial 300-mb. chart is shown in figure 4 which is quite similar to the 500-mb. surface (fig. 1) except for stronger winds and associated vorticity distributions.

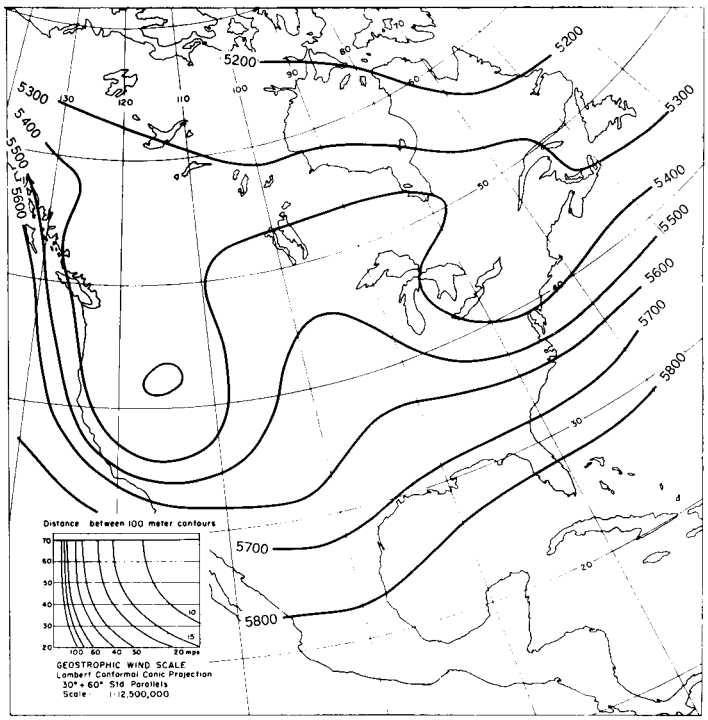

FIGURE 1.—Contours of the 500-mb. surface (unit meters) for December 31, 1200 GMT.

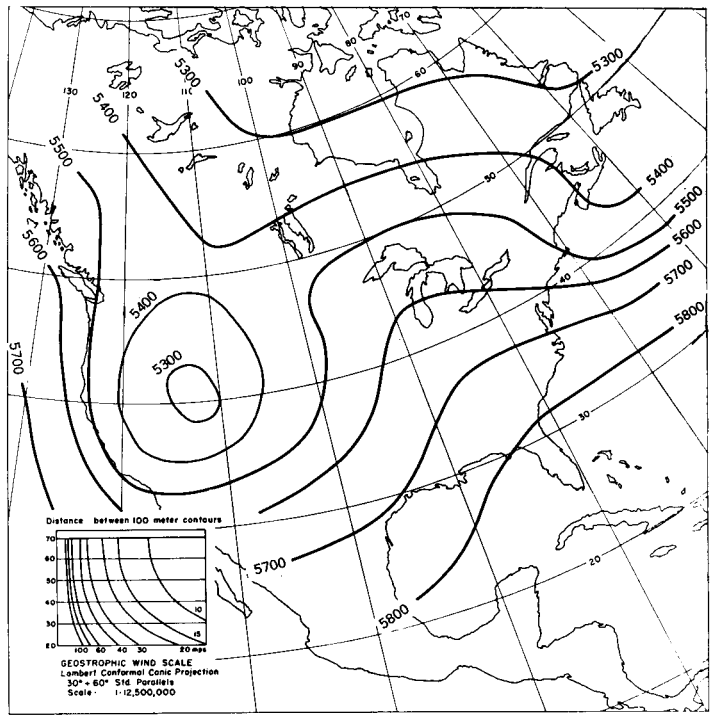

FIGURE 3.—24-hour barotropic forecast chart for the 500-mb. surface (unit meters) valid January 1, 1200 GMT.

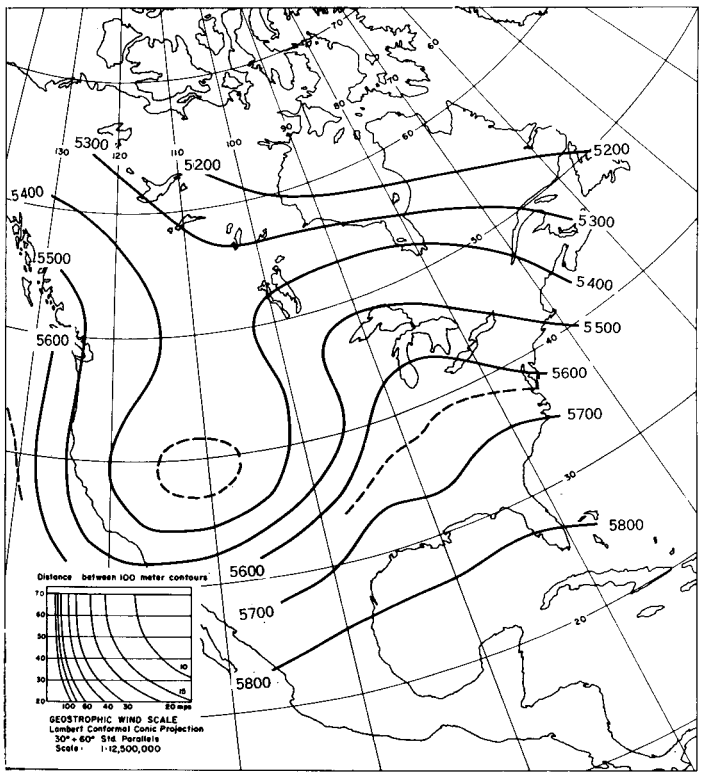

FIGURE 2.—Contours of the 500-mb. surface (unit meters) for January 1, 1200 GMT.

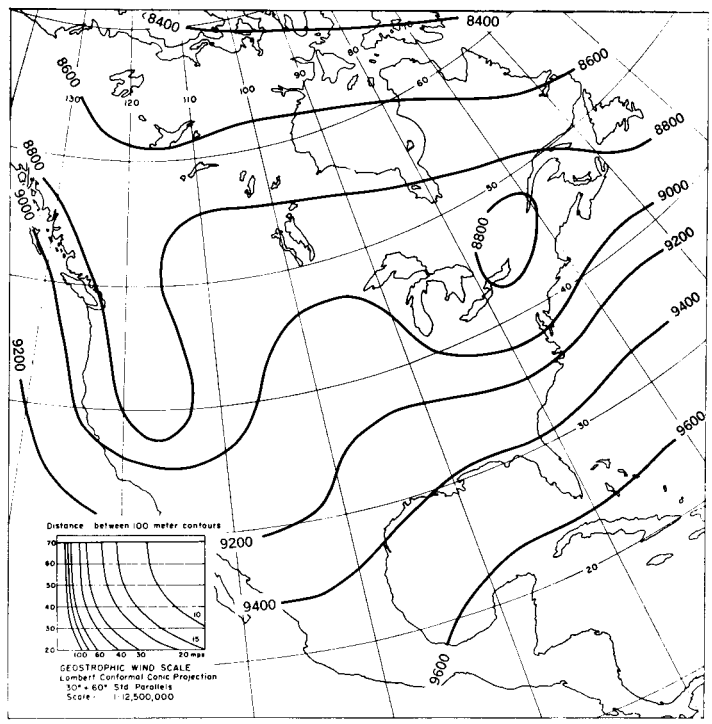

FIGURE 4.—Contours of the 300-mb. surface (unit meters) for December 31, 1200 GMT.

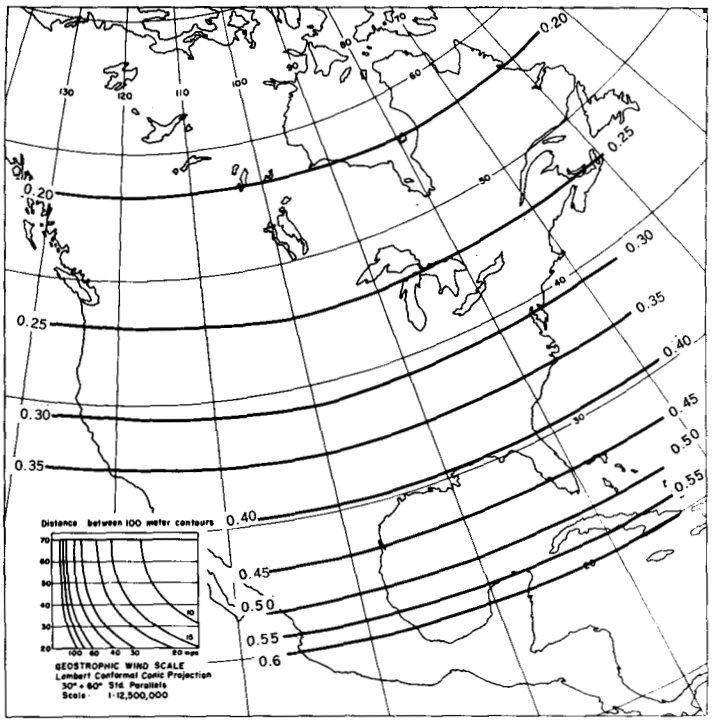

FIGURE 5.—Isolines of the quantity B (a non-dimensional parameter). B is a function of the latitude only.

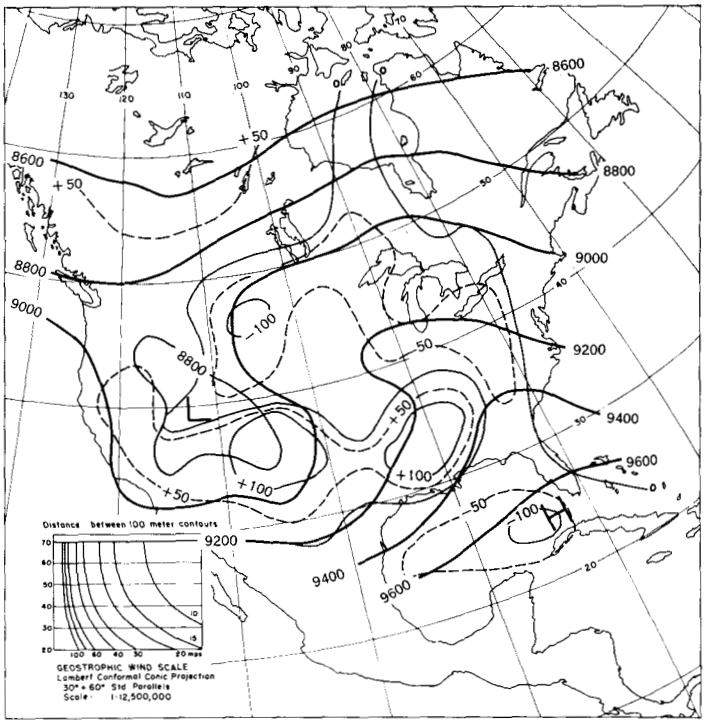

FIGURE 7.—Second approximation 24-hour graphical forecast for the 300-mb. surface, (unit meters) valid January 1, 1200 GMT. Also superimposed lines of the correction term demanded by the second approximation are shown in same units.

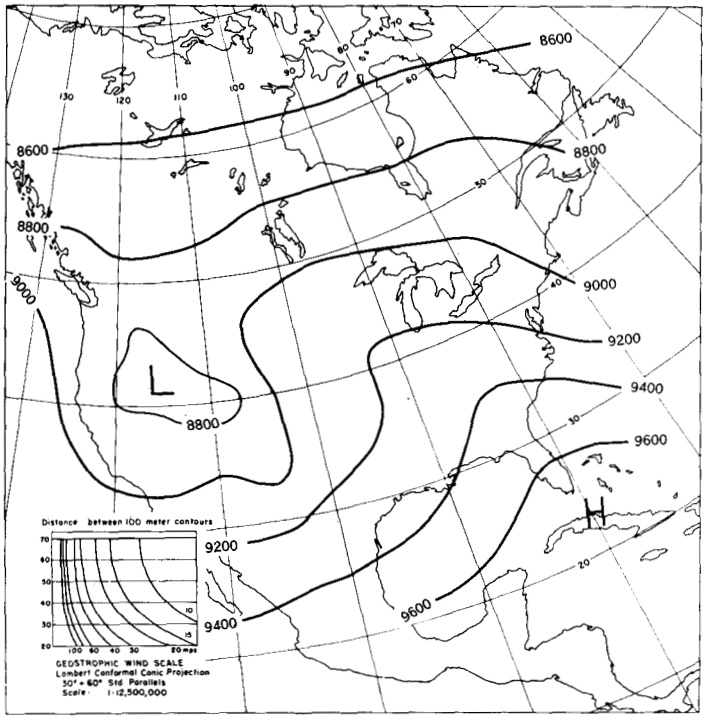

FIGURE 6.—First approximation 24-hour graphical forecast for the 300-mb. surface (unit meters) valid January 1, 1200 GMT.

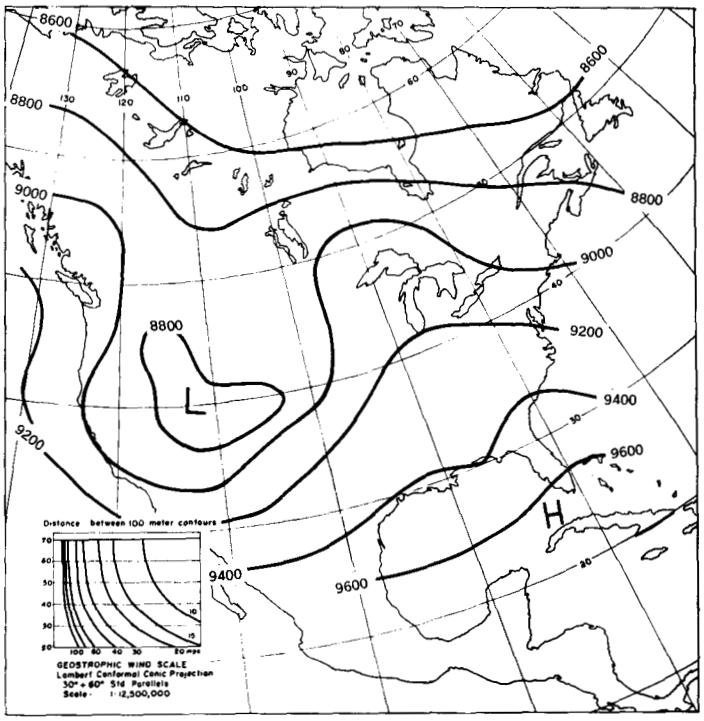

FIGURE 8.—The observed 300-mb. height for January 1, 1960, 1200 GMT (unit meters).

A subtropical jet is noticeable at this level with a core around 32° N. over the northern end of Florida. We shall not display the thickness charts or the charts of various estimated fields that were used in the analysis. A chart of the quantity B is shown in figure 5. We notice that it has a very small variation in the meridional direction, and is similar to the quantity G introduced by Fjørtoft in graphical smoothing for barotropic forecasting.

The 300-mb. forecast fields are shown in figures 6 and 7. These are respectively the first and second order approximations $z_F^{(1)}$ and $z_F^{(2)}$. The correction between the first and second order effects is superimposed in figure 7. The largest corrections are of the order of ± 100 meters. The principal regions of the corrections lie along the major wind belts, the subtropical and the polar jet streams where the shear term $(\mathbf{V}_1 - \mathbf{V}_2)$ is large. The isolated correction of -100 meters in the Gulf of Mexico also appears to be related to strong wind shears between the 500- and 300-mb. surfaces. Figure 7 appears to be a significant improvement on figure 6 in that the effect of vertical shear between the two levels has been incorporated.

It remains yet to compare figure 7 with the 300-mb. verification chart shown in figure 8. The observed change at the 300-mb. surface during the 24-hour period includes: deepening of the closed circulation at the trough, considerable weakening of the winds to the rear of the trough, and slow eastward movement of the other systems. The forecast shown by figure 7 appears to have described most of these observed features rather adequately.

The third order correction was carried out in the test exercise, but is not recommended as its contribution appeared small.

Forecast verifications are normally carried out with some mean square error estimation schemes. Using the following scheme

$$S^{(n)} = \sqrt{\frac{\int_y \int_x (z_{1F}^{(n)} - z_{01})^2 dx dy}{\int_y \int_x dx dy}}$$

Where the integrals are replaced by a summation over the entire area of calculation it was found that $S^{(2)}$ for the second approximation was about 25 meters less than $S^{(1)}$.

The third order approximation showed an insignificant improvement and $S^{(3)}$ and $S^{(2)}$ were almost identical.

6. FURTHER EXAMPLES

Only one other case has been investigated. The forecast made from January 1, 1960, 1200 GMT for January 2, 1960, 1200 GMT showed very similar results and hence the charts are not displayed here. It would perhaps be of interest to carry out such a procedure for varying initial conditions.

We shall next list the various steps of this iteration procedure.

7. MAIN STEPS IN THE GRAPHICAL FORECAST PROCEDURE

(i) Obtain 24-hour graphical forecast for z_2 by a barotropic forecasting model.

(ii) Assume conservation $(H^{(1)} - B\overline{H}^{(1)})$ and move the isopleths of this quantity along the two z_2 charts (initial and forecast).

(iii) Evaluate $H^{(1)}$ and $z_{1F}^{(1)}$ by the recovery equations (15) and (16).

(iv) Compute the Jacobean of the second term on the right of equation (14) by the advection procedure of Estoque. The term $\frac{f^2 B L^2}{4gm^2}$ is calculated once for all, $H^{(1)}$ and $z^{(1)}$ being given by step (iii).

(v) Add the correction demanded by step (iv) to the first term on the right of equation (14). The quantities $H^{(2)}$ and $z_{1F}^{(2)}$ are then recovered by step (iii).

The list given above does not contain the conventional details on moving charts; these are not listed because the operations may be found in any standard text book, such as Petterssen [7].

8. SOME CONCLUDING REMARKS

Graphical forecasting schemes will perhaps become a dying art if they are not pursued with the impetus with which they emerged in the literature since Fjørtoft's work in 1955. Perhaps the reason for a lack of general enthusiasm lies in the fact that one may accomplish the same purpose through the use of fast computers. The present work is an attempt to show the efficient working of a graphical forecast scheme that illustrates the basis of certain modern quasi-Lagrangian forecast methods. The time involved in carrying out such forecasts was found to be between one and two hours after careful planning.

The generality of equation (14) suggests its use for any two levels of the atmosphere, one of which is a level of non-divergence.

No attempt has been made to go into any theoretical aspects of the model. The baroclinic stability aspects of such a model have been discussed by Mihaljan [5]. Because of the wide use of two-level models in the research on numerical weather prediction, a graphical prediction analogue should be illustrative.

The 300-mb. forecasts made by this model suggest that the scheme is quite successful in producing reasonable results. Although only a limited number of cases has been tested so far, the author hopes to carry out a small sample of such forecasts for varying initial distributions.

ACKNOWLEDGMENT

The author wishes to convey his appreciation to Mr. George Neiiendam for general assistance in the preparation of this work. This work was initiated as an experiment for a graduate meteorology laboratory work and the contribution of the participants is acknowledged.

REFERENCES

1. M. A. Estoque, "Graphical Integrations of a Two-Level Model," *Journal of Meteorology*, vol. 14, No. 1, Feb. 1957, pp. 38–42.
2. R. Fjørtoft, "On a Numerical Method of Integrating the Barotropic Vorticity Equation," *Tellus*, vol. 4, No. 3, Aug. 1952, pp. 179–194.
3. R. Fjørtoft, "On the Use of Space-Smoothing in Physical Weather Forecasting," *Tellus*, vol. 7, No. 4, Nov. 1955, pp. 462–480.
4. E. Knighting, "Some Computations of the Variation of Vertical Velocity with Pressure on a Synoptic Scale," *Quarterly Journal of the Royal Meteorological Society*, vol. 86, No. 369, July 1960, pp. 318–325.
5. J. M. Mihaljan, "The Baroclinic Instability of a '2½ Dimensional Model Atmosphere' in Which the Upper Level Is Non-Divergent," *Technical Report*, Armour Research Foundation of Illinois Institute of Technology, 1961.
6. H. Oakland, "An Experiment in Numerical Integration of the Barotropic Equation by a Quasi-Lagrangian Method," *Geofysiske Publikasjoner*, vol. 22, No. 5, 1962, pp. 1–10.
7. S. Petterssen, *Weather Analysis and Forecasting*, vol. 1, McGraw-Hill Book Company, Inc., New York, 1956, 428 pp. (See p. 388).
8. R. J. Reed, "A Graphical Method for Preparing 1000 Millibar Prognostic Charts," *Journal of Meteorology*, vol. 14, No. 1, Feb. 1957, pp. 65–70.
9. J. S. Sawyer, "Experiments in Integrating the Vorticity Advection Equation by a Lagrangian Method," *Technical Note* (B), Meteorological Office, Dunstable, England, 1960.
10. A. Wiin-Nielsen, "On the Application of Trajectory Methods in Numerical Forecasting," *Tellus*, vol. 11, No. 2, May 1959, pp. 180–196.